KALMAN FILTERING WITH UNLIMITED SENSING

Hongwei Wang* Xi Zheng* Hongbin Li[†]

* University of Electronic Science and Technology of China, Chengdu 611731, China

† Stevens Institute of Technology, Hoboken 07030, USA

ABSTRACT

In this paper, we consider state estimation in the Kalman filtering framework with unlimited sensing measurements (USMs), which are obtained from sensors equipped with a self-reset analog-to-digital (SR-ADC). SR-ADC was recently introduced to deal with the saturation issue frequently encountered in a conventional ADC. To tackle the nonlinearity of the USM, we present a unique decomposition property of the USM. Leveraging this property and a multiple model adaptive estimation strategy, we propose a novel USF-based Kalman filtering (KF-USM) algorithm. Numerical results reveal that the proposed KF-USM filter is an effective alternative to the conventional ADC-based KF to deal with high dynamic range input signals, offering more accurate state estimation in the presence of saturation.

Index Terms— Kalman filtering, multiple models, unlimited sensing

1. INTRODUCTION

The Kalman filter (KF) [1] and its nonlinear variants [2–4] are ubiquitous tools to estimate the state of dynamic state-space models (SSM), which are employed in various applications including target tracking [5], fault detection and diagnosis [6], system identification [7], adaptive feedback cancellation [8], and many others. In such applications, each sensor is equipped with an analog-to-digital converter (ADC) to convert the analog observed signal to digital. However, saturation occurs when the amplitude of the input signal exceeds the dynamic range of the ADC, leading to a censored measurement, which may result in significant performance degradation of the KF and its nonlinear extensions.

To cope with the censored measurements, a Tobit KF (TKF) is proposed in [9], via a Tobit model, for state estimation. In the TKF, the likelihood function of an observation is modified so that it can reflect the probability that the corresponding variable is above or below the censored threshold. Although TKF helps increase

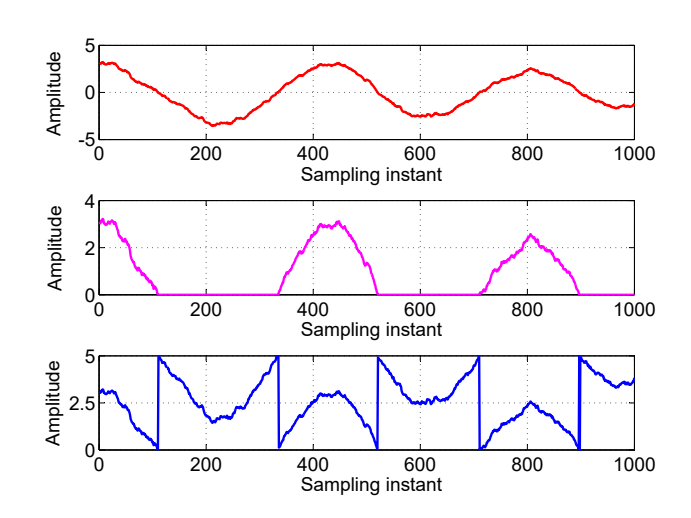


Fig. 1: Measurements from sensors with an ideal ADC (top); a conventional ADC that can only record positive values (middle); a SR-ADC (bottom).

the estimation accuracy, the so-obtained improvement in estimation accuracy is limited due to the permanent loss of information in censored observations.

The recently introduced unlimited sensing framework [10] offers an alternative approach to addressing the above drawback of conventional measurement range-limited ADCs. The unlimited sensing is a hardware-software co-design approach. The core idea of unlimited sensing is to utilize a self-reset ADC (SR-ADC) to fold an arbitrary input signal into the recordable range by taking a modulo related operation. We provide a comparison of measurements from a sensor with a conventional ADC (the middle of Fig. 1) and measurements from a sensor with a SR-ADC (the bottom of Fig. 1) when the input signal is shown in the top of Fig. 1. It can be seen that, when the output exceeds the operation range of the ADC, the SR-ADC saves the information via a modulo operation, while the conventional ADC simply sets the output to its threshold (i.e., 0 in Fig. 1).

However, the resulting unlimited sensing measurement (USM) creates a challenge in signal processing, since the input/output relationship of the SR-ADC is highly

This research was supported by the National Natural Science Foundation of China under Grants No. 62103083. The work of H. Li was supported in part by the National Science Foundation under Grants ECCS-1923739, ECCS-2212940, and CCF-2316865.

nonlinear. Several applications have been investigated over the past few years, including the estimation of sinusoidal mixtures [11], direction-of-arrival estimation [12], sparse signal recovery [13], and others. In this work, we extend the application of the USM to the estimation of the dynamic SSMs and propose a novel filtering algorithm to estimate the state of interest. To tackle the nonlinearity of the USM, we propose a novel Kalman filter by exploiting a unique decomposition of the USM and a multiple model adaptive estimation (MMAE) based strategy. Simulation results reveals that the proposed method can provide accurate state estimates in the presence of high dynamic range input signals, illustrating the effectiveness of using SR-ADC and USM in replacement of the conventional ADC.

2. PROBLEM FORMULATION

Consider a linear dynamic system with state evolution as

$$\boldsymbol{x}_t = \boldsymbol{F} \boldsymbol{x}_{t-1} + \boldsymbol{w}_t \tag{1}$$

where $x_t \in \mathbb{R}^n$ is the state of interest at time instant t, F is a known state transmission matrix, and $w_t \sim \mathbb{N}(0, Q_t)$ is the process noise. Ideally, the state of such a dynamic system is observed via

$$y_t = Hx_t + v_t \tag{2}$$

where v_t is the Gaussian measurement noise with zero-mean and covariance R_t .

However, the amplitude of \boldsymbol{y}_t may exceed the operation range of the sensor, resulting in censoring/saturation. To avoid this issue, a self-reset analog-to-digital (SR-ADC) device is employed at the measurement sensor to fold the out-of-range amplitudes into a recordable range. Specifically, the output of the dynamic system is expressed as

$$\boldsymbol{z}_{t} = \mathcal{U}_{\lambda} \left(\boldsymbol{y}_{t} \right) = \mathcal{U}_{\lambda} \left(\boldsymbol{H} \boldsymbol{x}_{t} + \boldsymbol{v}_{t} \right) \tag{3}$$

where $\mathcal{U}_{\lambda}(\cdot)$ is an element-wise nonlinear mapping. For a scalar $a, \mathcal{U}_{\lambda}(a)$ is defined as

$$\mathcal{U}_{\lambda}(a): a \mapsto \lambda \left(\frac{a}{\lambda} - \left\lfloor \frac{a}{\lambda} \right\rfloor\right)$$
 (4)

where $\lambda \geq 0$ is the dynamic range of the sensor, and $\lfloor a \rfloor$ denotes the floor function. It is apparent that (4) folds back an arbitrary vale a into the interval $[0,\lambda]$, and hence we hereafter call such a measurement as the USM.

Remark: It should be noticed that in most existing works, the nonlinear mapping related to the sensor with a SR-ADC is given as

$$\mathcal{U}_{\lambda}(a): a \mapsto 2\lambda \left(\frac{a}{2\lambda} - \left\lfloor \frac{a}{\lambda} + \frac{1}{2} \right\rfloor \right)$$

which folds back an arbitrary vale a into a symmetric interval $[-\lambda, \lambda]$. In this work, we consider the asymmetric one in (4)

for ease of comparison with the TKF. The proposed filtering algorithm can be easily extended to the symmetric case.

The objective of this work is to estimate the state of interest based on the measurements $\{z_t\}_{t=1}^T$. Theoretically, existing nonlinear filtering algorithms such as the Gaussian approximation filters and particle filter (PF) can be utilized to obtain the estimates of the states. However, these approaches ignore the inherent property of the nonlinear mapping, which would incur performance degradation.

3. MULTIPLE MODEL BASED SOLUTION

3.1. Representation of The USM

The nonlinear mapping involved in the USM makes the filtering problem more challenging. To deal with this issue, we introduce the following proposition concerning the unique decomposition of the USM.

Proposition 1. If $z = \mathcal{U}_{\lambda}(a)$, where λ is a fixed and positive constant, then the relationship between z and a is given by

$$z = a + \lambda e \tag{5}$$

where e is an integer that can be uniquely determined for given a and λ .

This proposition can be easily proved by the definition in (4). Specifically, we know that

$$z = \lambda \left(\frac{a}{\lambda} - \left\lfloor \frac{a}{\lambda} \right\rfloor \right) = a - \lambda \left\lfloor \frac{a}{\lambda} \right\rfloor \tag{6}$$

Comparing (5) and (6), we can conclude that $e = -\lfloor a/\lambda \rfloor$, which is an integer with a unique value.

Based on the unique decomposition in (5) and the fact that $U_{\lambda}(a)$ is an element-wise mapping, we can rephrase (3) as

$$z_t = Hx_t + v_t + \lambda e \tag{7}$$

where $e \in \mathbb{Z}^m$ is a vector with each element being an integer.

3.2. Kalman Filtering with The USM

In this section, we employ a multiple model adaptive estimation (MMAE) algorithm to estimate the state of interest. In the MMAE framework, a finite set of models from prior knowledge is provided, and the true model is assumed to be (or at least can be adequately approximated by) one of these models. In our problem, the set of models can be formulated as

$$\boldsymbol{x}_t = \boldsymbol{F} \boldsymbol{x}_{t-1} + \boldsymbol{w}_t \tag{8}$$

$$\boldsymbol{z}_t = \boldsymbol{H}\boldsymbol{x}_t + \boldsymbol{e}^p \lambda + \boldsymbol{v}_t, \ (p = 1, \cdots, P)$$
 (9)

where e^p denotes the integer vector for the pth model, and P is the number of models. From Section 3.1 we know that P is

theoretically tending to infinity, which effectively renders the MMAE framework inapplicable. To deal with this issue, we utilize the predicted value of the state to reduce P to a finite number. The details of the proposed Kalman filter with the USM based on the MMAE framework is described as follows.

Step 1: State Prediction.

The prediction step of the proposed Kalman filtering algorithm is the same as the conventional one. Specifically, given the estimated state $\hat{x}_{t-1|t-1}$ and its associated with error covariance matrix P_{t-1} , we have

$$\hat{x}_{t|t-1} = F_t \hat{x}_{t-1|t-1} \tag{10}$$

$$P_{t|t-1} = F_t^T P_{t-1} F_t + Q_{t-1}$$
 (11)

Step 2: Determining P and $\{e^p\}$.

Using the predicted state, we can calculate the estimate value of $\boldsymbol{H}\boldsymbol{x}_t$ as $\boldsymbol{H}\boldsymbol{\hat{x}}_{t|t-1}$, which can be further utilized to estimate the integer vector \boldsymbol{e} . Specifically, the ith component of \boldsymbol{e} can be provided as

$$\hat{e}_i = \left| \frac{(\boldsymbol{z}_t - \boldsymbol{H} \hat{\boldsymbol{x}}_{t|t-1})_i}{\lambda} \right| \tag{12}$$

where $(a)_i$ denotes the *i*th element of the vector a. Although \hat{e}_i may not be exactly the same as the true value e_i due to the existence of the measurement noise, these two values are very close. Therefore, we can assume that e_i belongs to the set Ξ_i

$$e_i \in \Xi_i \triangleq \{e_i | |e_i - \hat{e}_i| \le K, e_i \in \mathbb{Z}, K \in \mathbb{Z}_+\}$$
 (13)

where K is a positive integer. It is apparent that e_i has 2K+1 possible values. In addition, we define Σ as a set that contains all possible combinations of $\{e_i\}_{i=1}^m$, i.e.,

$$\Sigma \triangleq \left\{ \boldsymbol{e} = [e_1, \cdots, e_m]^T | e_i \in \Xi_i, i \in \{1, \cdots, m\} \right\}$$
 (14)

We choose $e_p \in \Sigma$, and hence P can be determined by the candidate of Σ , which is given by

$$P = (2K+1)^m (15)$$

Step 3: Filtering for Each Individual Model.

Once P and $\{e^p\}$ are obtained, we can implement the standard measurement update for each individual model in parallel. Specifically, for the pth model, we have

$$\hat{\boldsymbol{x}}_{t|t}^{p} = \hat{\boldsymbol{x}}_{t|t-1} + \boldsymbol{K}(\boldsymbol{z}_{t} - \boldsymbol{H}\hat{\boldsymbol{x}}_{t|t-1} - \boldsymbol{e}^{p}\boldsymbol{\lambda})$$
 (16)

$$K^{p} = P_{t|t-1}H^{T}(HP_{t|t-1}H^{T} + R_{t})^{-1}$$
 (17)

$$\boldsymbol{P}_{t}^{p} = (\boldsymbol{I} - \boldsymbol{K}^{p} \boldsymbol{H}) \boldsymbol{P}_{t|t-1}$$
(18)

It should be noted that the measurement update procedure for each model has the same Kalman gain and the filtered covariance.

Step 4: Calculating Probability for Each Model.

The residual vector for each model is defined as

$$\tilde{\boldsymbol{z}}_t^p \triangleq \boldsymbol{z}_t - \boldsymbol{H}\hat{\boldsymbol{x}}_{t|t-1} - \boldsymbol{e}^p \lambda \tag{19}$$

and its corresponding covariance matrix is given by

$$S = HP_{t|t-1}H^T + R_t \tag{20}$$

Theoretically, if the pth model is the true model, \tilde{z}_t^p follows the Gaussian distribution $\mathbb{N}(\mathbf{0}, \mathbf{S})$. Therefore, the conditional probability of each model is given by

$$\mu_p = \frac{\kappa_p}{\sum_{p=1}^P \kappa_p} \tag{21}$$

where κ_p is calculated by the Gaussian likelihood

$$\kappa_p = \frac{1}{(|2\pi \mathbf{S}|)^{0.5}} \exp\left(-\frac{1}{2}(\tilde{\mathbf{z}}_t^p)^T \mathbf{S}^{-1} \tilde{\mathbf{z}}_t^p\right)$$
(22)

Step 5: Obtaining The Estimate of The State.

The filtered state and its corresponding covariance is obtained by combining the estimated results of each model, i.e.,

$$x_{t|t} = \sum_{p=1}^{P} \mu_p \hat{x}_{t|t}^p, \ P_t = \sum_{p=1}^{P} \mu_p P_t^p$$
 (23)

It should be noticed that the update procedure in *Step 5* is different from the one in the interacting multiple model Kalman filter [14]. This is because the multiple models in our approach are independent and there is not an interacting procedure.

4. SIMULATION RESULTS

In this section, numerical simulations are employed to illustrate the performance of the proposed Kalman filter with USM (KF-USM)¹. We consider a linear dynamic system [9]

$$\begin{bmatrix} x_{t,1} \\ x_{t,2} \end{bmatrix} = \begin{bmatrix} \cos(\theta) & -\sin(\theta) \\ \sin(\theta) & \cos(\theta) \end{bmatrix} \begin{bmatrix} x_{t-1,1} \\ x_{t-1,2} \end{bmatrix} + \begin{bmatrix} w_{t,1} \\ w_{t,2} \end{bmatrix}$$
(24)

$$y_t = \begin{bmatrix} 1 & 0 \end{bmatrix} \begin{bmatrix} x_{t,1} \\ x_{t,2} \end{bmatrix} + v_t \tag{25}$$

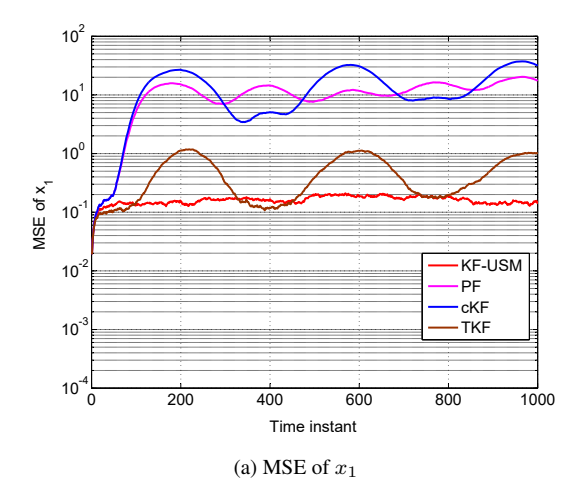
where $\boldsymbol{x}_t \triangleq [x_{t,1}, x_{t,2}]^T$ is the state of interest, θ is a system parameter, $\boldsymbol{w}_t \triangleq [w_{t,1}, w_{t,2}]^T \sim \mathbb{N}(\boldsymbol{0}, \boldsymbol{Q}_t)$ is the process noise, and $v_t \sim \mathbb{N}(0, R_t)$. The USM is given by

$$z_t = \mathcal{U}_{\lambda}(y_t) \tag{26}$$

We compare the KF-USM with the conventional KF (cKF) and the PF. In addition, the TKF is also compared, and the censoring measurement model of the TKF is given by

$$z_t = \begin{cases} y_t, & y_t > 0\\ 0, & y_t \le 0 \end{cases} \tag{27}$$

¹Simulation codes and data can be found in: https://github.com/tianhangnpu/KF_US_ICASSP2024.



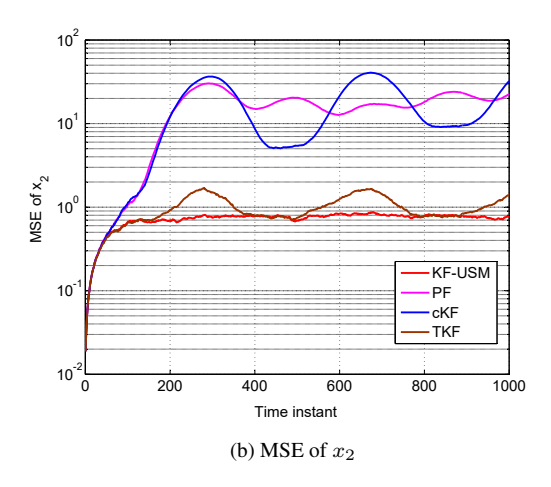


Fig. 2: The MSEs of the compared methods.

To evaluate the performance of different filters, the mean squared error (MSE) at each instant t is employed as a metric, which is defined as (taking $x_{t,1}$ as an example)

$$MSE(t) = \frac{1}{L} \sum_{l=1}^{L} (x_{t,1}^{l} - \hat{x}_{t,1}^{l})^{2}, \quad t = 1, \dots, T$$
 (28)

where L is the number of independent Monte Carlo runs, and $x_{t,1}^l$ and $\hat{x}_{t,1}^l$, respectively, denote the true and estimated state component at time t in the lth Monte Carlo run.

In simulations, we set $\theta = 0.0052\pi$, $Q_{t-1} = 0.01I_2$ and $R_t = 1$, $\lambda = 5$. The initial state $x_{0,1}$ and $x_{0,2}$ are randomly selected from $\mathbb{N}(\boldsymbol{x}_0, 0.01I_2)$ where $\boldsymbol{x}_0 = [3, 0]^T$. The simulation results are obtained via L = 1000 Monte Carlo runs. In the PF, we set the number of particles to 1000.

Fig. 2 illustrates the performance of the compared methods in the RMSE sense, and Fig. 3 presents the estimated x_1 in a certain Monte Carlo run. It can be seen that both the KF-USM and the TKF have relatively small RMSEs compared with the cKF and the PF. Meanwhile, in the considered simulation run, we can see that the cKF (at the

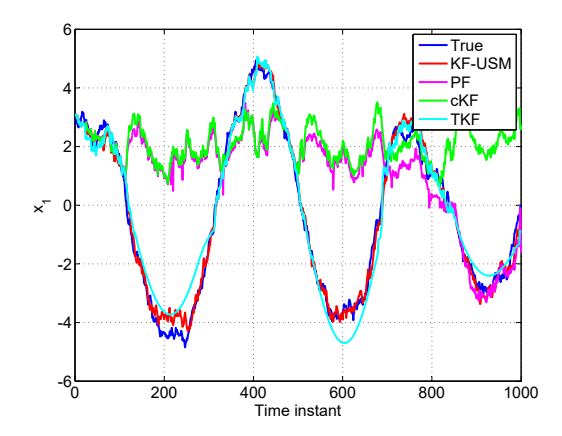


Fig. 3: The true and estimated x_1 in a specific Monte Carlo run.

initial stage) and the PF (and the initial and the ending stages) can only partially track the state of x_1 , while both the KF-USM and the TKF can correctly follow the trend of x_1 . Therefore, we can conclude that both the KF-USM and the TKF have significant performance improvements compared with the cKF and the PF. Hence, taking the additional information of the saturated measurements or the folded measurements into account can indeed enhance the estimation accuracy.

In addition, although both outperforming others, the KF-USM is superior to the TKF. This is because, the USM essentially encodes information of the data into its modulo, while the sensor with a conventional ADC only records the maximum (or the minimum) range of the ADC and the details are lost. Apparently, the sensor in the unlimited sensing framework has an advantage over the sensor with a conventional ADC.

5. CONCLUSIONS

We studied the Kalman filtering problem in an unlimited sensing framework, in which measurements are obtained via a sensor equipped with a SR-ADC to avoid saturation. We proposed a MMAE based Kalman filter for the USM, and the multiple measurement models were constructed by a unique decomposition property of the USM. Simulation results show that the proposed method can provide reliable state estimates, and that the unlimited sensing framework has an advantage over the conventional solutions when dealing with saturations. The computational complexity of the proposed method is exponential in the dimension of the measurement. Therefore, how to reduce the computational complexity is one of the future research directions.

6. REFERENCES

- [1] Rudolph Emil Kalman, "A new approach to linear filtering and prediction problems," *Journal of Basic Engineering*, vol. 82, no. 1, pp. 35–45, 1960.
- [2] Eric A Wan and Rudolph Van Der Merwe, "The unscented kalman filter for nonlinear estimation," in Proceedings of the IEEE 2000 Adaptive Systems for Signal Processing, Communications, and Control Symposium (Cat. No. 00EX373). Ieee, 2000, pp. 153– 158.
- [3] M Sanjeev Arulampalam, Simon Maskell, Neil Gordon, and Tim Clapp, "A tutorial on particle filters for online nonlinear/non-gaussian bayesian tracking," *IEEE Transactions on Signal Processing*, vol. 50, no. 2, pp. 174–188, 2002.
- [4] Hongwei Wang, Wei Zhang, Junyi Zuo, and Heping Wang, "Generalized cubature quadrature kalman filters: derivations and extensions," *Journal of Systems Engineering and Electronics*, vol. 28, no. 3, pp. 556–562, 2017.
- [5] Ronghui Zhan and Jianwei Wan, "Iterated unscented Kalman filter for passive target tracking," *IEEE Transactions on Aerospace and Electronic Systems*, vol. 43, no. 3, pp. 1155–1163, 2007.
- [6] Weihua Li, Sirish L Shah, and Deyun Xiao, "Kalman filters in non-uniformly sampled multirate systems: For FDI and beyond," *Automatica*, vol. 44, no. 1, pp. 199– 208, 2008.
- [7] Yuanyuan Liu, Hongwei Wang, and Wei Zhang, "Robust parameter estimation with outlier-contaminated correlated measurements and applications to aerodynamic coefficient identification," *Aerospace Science and Technology*, vol. 118, pp. 106995, 2021.
- [8] Felix Albu, Linh TT Tran, and Sven Nordholm, "The hybrid simplified Kalman filter for adaptive feedback cancellation," in 2018 International conference on communications (COMM). IEEE, 2018, pp. 45–50.
- [9] Bethany Allik, Cory Miller, Michael J Piovoso, and Ryan Zurakowski, "The tobit kalman filter: an estimator for censored measurements," *IEEE Transactions on Control Systems Technology*, vol. 24, no. 1, pp. 365–371, 2015.
- [10] Ayush Bhandari, Felix Krahmer, and Ramesh Raskar, "On unlimited sampling and reconstruction," *IEEE Transactions on Signal Processing*, vol. 69, pp. 3827–3839, 2020.

- [11] Ayush Bhandari, Felix Krahmer, and Ramesh Raskar, "Unlimited sampling of sparse sinusoidal mixtures," in 2018 IEEE International Symposium on Information Theory (ISIT). IEEE, 2018, pp. 336–340.
- [12] Samuel Fernández-Menduiña, Felix Krahmer, Geert Leus, and Ayush Bhandari, "Computational array signal processing via modulo non-linearities," *IEEE Transactions on Signal Processing*, vol. 70, pp. 2168– 2179, 2022.
- [13] Ayush Bhandari, Felix Krahmer, and Ramesh Raskar, "Unlimited sampling of sparse signals," in 2018 IEEE International Conference on Acoustics, Speech and Signal Processing (ICASSP). IEEE, 2018, pp. 4569– 4573.
- [14] Efim Mazor, Amir Averbuch, Yakov Bar-Shalom, and Joshua Dayan, "Interacting multiple model methods in target tracking: a survey," *IEEE Transactions on Aerospace and Electronic Systems*, vol. 34, no. 1, pp. 103–123, 1998.